Coulomb-driven band unflattening suppresses K-phonon pairing in moiré graphene

Glenn Wagner [1] Yves H. Kwan,[2] Nick Bultinck,[3,4] Steven H. Simon,[3] and S. A. Parameswaran [3]

[1]*Department of Physics, University of Zurich, Winterthurerstrasse 190, 8057 Zurich, Switzerland*
[2]*Princeton Center for Theoretical Science, Princeton University, Princeton, New Jersey 08544, USA*
[3]*Rudolf Peierls Centre for Theoretical Physics, Parks Road, Oxford OX1 3PU, United Kingdom*
[4]*Department of Physics, Ghent University, Krijgslaan 281, 9000 Gent, Belgium*

It is a matter of current debate whether the gate-tunable superconductivity in twisted bilayer graphene is phonon mediated or arises from electron-electron interactions. The recent observation of the strong coupling of electrons to so-called K-phonon modes in angle-resolved photoemission spectroscopy experiments has resuscitated early proposals that K phonons drive superconductivity. We show that the bandwidth-enhancing effect of interactions drastically weakens both the intrinsic susceptibility towards pairing as well as the screening of Coulomb repulsion that is essential for the phonon attraction to dominate at low temperature. This rules out purely K-phonon-mediated superconductivity with the observed transition temperature of ~ 1 K. We conclude that the unflattening of bands by Coulomb interactions challenges any purely phonon-driven pairing mechanism, and must be addressed by a successful theory of superconductivity in moiré graphene.

I. INTRODUCTION

Superconductivity (SC) requires attractive interactions between electrons to form Cooper pairs. In conventional SC, the necessary "glue" is provided by phonons, but pairing can arise in other ways, ranging from the exchange of collective excitations to "overscreening" of Coulomb interactions, as in the Kohn-Luttinger mechanism [1]. A case in point is the cuprate high-temperature superconductors: Their phenomenology is widely thought to be inconsistent with phonon-mediated pairing, leading to extensive efforts to explain the origin of their high transition temperatures (T_c).

Since the discovery of gate-tunable SC in twisted bilayer graphene (TBG) [2–8], the pairing mechanism and its similarity to that in the cuprates has been debated. The highest reported T_c in TBG is around 3 K [8], which is high compared to the Fermi temperature. This has motivated several theories of Coulomb-interaction-mediated SC [9–29], whereas the myriad peculiarities of the moiré superlattice structure and electronic band topology have stimulated a comparable number of proposals for phonon-mediated mechanisms [17,30–43].

Experimentally, there are hints that phonons may drive SC in TBG. Increasing the screening of the Coulomb interaction in TBG is shown to suppress the correlated insulators, while leaving T_c relatively unchanged [44–46]. Furthermore, recent angle-resolved photoemission spectroscopy (ARPES) experiments have observed strong coupling of the electrons to a K-phonon mode [47] and that SC is absent in devices where coupling to this mode appears to be suppressed.

Two existing theoretical proposals for SC consider K-phonon-mediated pairing [32,33]; however, the corresponding energy scale (~ 0.5 meV) is weak compared to the repulsive Coulomb interaction (~ 20 meV). The effectiveness of K-phonon pairing therefore relies on the screening of the Coulomb interaction due to the high density of states in the central bands of TBG. Theoretically incorporating screening at the Thomas-Fermi (TF) level and working with the narrow (~ 1 meV bandwidth) bands of the Bistritzer-MacDonald (BM) model [48], Refs. [32,33] indeed find K-phonon-mediated SC with $T_c \sim 1$ K, that compares favorably with experiment.

However, scanning tunneling microscopy (STM) [49–52], compressibility [53], and ARPES [54] experiments indicate that the bandwidth of the central bands is significantly larger (~ 50 meV) than that of the bare noninteracting BM model. This "band unflattening" is likely due to both the interaction-induced renormalization of the band structure as well as the effect of strain, known to be important in TBG [55–58]. The increased bandwidth lowers the density of states, both weakening the pairing instability and suppressing screening. How does this impact K-phonon SC?

We answer this question by studying the pairing of electrons in the Hartree-Fock (HF) renormalized bands of TBG, in the presence of Thomas-Fermi screened Coulomb interactions and K-phonon attraction. We show that in any realistic parameter regime, the enhancement of the bandwidth and suppression of the density of states leads to a significant reduction of T_c to well below experimentally reported values. We find similar results irrespective of whether electrons are doped into the incommensurate Kekulé spiral state known to be the ground state at nonzero integer filling and nonzero strain, the strong-coupling "ferromagnetic" insulators at zero strain, or the gapless parent states of either phase: Band unflattening is the key to suppressing T_c. Our results show that theories of phonon-mediated attraction in TBG must include screening beyond the Thomas-Fermi approximation, or identify another route to evade the Coulomb suppression of pairing.

II. HARTREE-FOCK BAND STRUCTURE

The starting point for many studies of TBG are the BM bands, computed using the noninteracting continuum model

of Ref. [48]. We also begin here, choosing as BM parameters sublattice-dependent hopping matrix elements $w_{AB} = 110$ meV and $w_{AA} = 80$ meV, and a twist angle $\theta = 1.1°$, corresponding to a bare bandwidth ~ 1 meV. However, our next step is less commonly pursued: We consider the enhancement of the bandwidth by Coulomb interactions. We study this effect, expected to be significant, using the self-consistent HF approximation. HF has been successfully used to make a variety of nontrivial quantitative predictions in TBG [56,57,59–70], and is expected to capture well the interaction-driven broadening of the bandwidth. To match the experimental device setting, we assume a dual-gate screened Coulomb interaction $V^0(q) = e^2 \tanh(qd)/(2\epsilon_0\epsilon_r q)$ with $\epsilon_r = 10$ and gate distance $d = 25$ nm. We use the so-called "average" subtraction scheme to avoid double counting the interactions (see Ref. [57] for details). To obtain the interaction-renormalized band structure, we perform a self-consistent HF calculation on a 10×10 grid for the moiré Brillouin zone (mBZ), and then interpolate the resulting bands following the procedure described in Ref. [71] to a 40×40 grid (for solving the SC gap equation) and a 100×100 grid (to compute the density of states).

III. *K* PHONONS, SCREENING, AND THE GAP EQUATION

TBG hosts a variety of phonon modes; both acoustic phonons and phasons experience strong moiré effects and both have been proposed as drivers of SC. However, there are other graphene phonon modes that are very strongly coupled to the moiré bands. Motivated by the recent observation of a particularly strong coupling of the central-band electrons to the A_1 zone-corner optical phonon mode [47], we focus here on pairing due to this "K-phonon" mode. K-phonon coupling can favor different insulating states [39] and in Ref. [72] it has been mooted as a route to stabilizing the Kekulé charge order seen in STM on ultralow strain samples [73]. The corresponding phonon-induced electron-electron interaction is

$$H_{ph} = -g \sum_l \int d^2r [(\psi_l^\dagger \tau_x \sigma_x \psi_l)^2 + (\psi_l^\dagger \tau_y \sigma_x \psi_l)^2], \quad (1)$$

where ψ is a spinor in sublattice space, l is the layer index, σ_i (τ_i) are Pauli matrices in sublattice (valley) space, and g is the coupling constant $\simeq 69$ meV nm^2 [32]. Two previous studies have considered K-phonon mediated SC: Ref. [32] finds a maximum T_c of around 10 K in the noninteracting problem; Ref. [33] incorporates Thomas-Fermi screened Coulomb repulsion and finds that this reduces T_c to around 2 K. These results appear consistent with the experimental T_c of around 1–3 K. However, crucially—as already pointed out in Ref. [33]—this is likely an overestimate of T_c since both these works solve the gap equation for the BM model at the magic angle, which has an extremely small bandwidth. The interaction scale in TBG is large compared to the bandwidth; accounting for the former via HF yields a significant enhancement of the latter, consistent with experimental measurements, renormalization group (RG) studies [74], and quantum Monte Carlo studies [75]. Both suggest that the actual bandwidth is least an order of magnitude larger than that of the magic-angle BM model. Therefore, instead of starting from the BM band structure, a more accurate approach is

TABLE I. Six band structures investigated. We list the six band structures that we considered as the parent state for SC. The band structures have different symmetries enforced [the symmetries being a subset of C_3 rotation, spin SU(2), valley $U_V(1)$, and time reversal $\mathcal{T}$]. We list the symmetries which are either broken (✗) or preserved (✓) by each band structure. In the case of C_3 we also list whether the symmetry is broken spontaneously (S) or explicitly (E).

Band structure (symmetries enforced)	Strain	C_3	SU(2)	$U_V(1)$	$\mathcal{T}$
(a) BM	✓	✓	✓	✓	✓
(b) HF (C_3+flavor)	✓	✓	✓	✓	✓
(c) HF (flavor)	✓	✗(S)	✓	✓	✓
(d) HF	✓	✗(S)	✗	✗	✗
(e) HF (flavor)	0.3%	✗(E)	✓	✓	✓
(f) HF	0.3%	✗(E)	✗	✗	✓

to solve the gap equation for the HF band structure as we now do. Besides the phonon-mediated attraction, we can also incorporate screened repulsive Coulomb interactions,

$$V(q) = \frac{V^0(q)}{1 - \Pi(q)V^0(q)}, \quad (2)$$

where we make the TF approximation $\Pi(q) \approx -D(E_F)$. As we note in the discussion below, it is in principle possible though technically much more demanding to account for screening in a more refined manner, e.g., by computing the polarization bubble in the random-phase approximation (RPA). This may allow effects such as overscreening which may be able to seed superconductivity. However, the numerical challenge in implementing these extensions renders them beyond the scope of the present paper. Other authors have performed such calculations and found them to be a viable route towards superconductivity in TBG [9,24,29,76]. We note that for acoustic phonons, which we do not consider here, there can be additional screening from the Anderson-Morel mechanism [37,77].

For a given band structure, we solve the gap equation

$$\Delta_{ab}(k) = -\frac{1}{A} \sum_{k',cd} U_{abcd}(k,k') \pi_{cd}(k') \Delta_{cd}(k'), \quad (3)$$

where roman letters indicate a band label, and $U_{abcd}(k,k')$ is the BCS-channel vertex—either a purely phonon attraction or contains both a phonon and Coulomb contribution. Since the gap equation is a mean-field result, there will be no superconducting solution for a positive definite interaction such as the bare Coulomb interaction without phonons [78]. $\pi_{cd}(k')$ is the particle-particle susceptibility. At low temperatures, π is sharply peaked at the Fermi surface. We therefore evaluate the momentum sum on a set of momentum points obtained via importance sampling from the susceptibility [79]. We solve the gap equation at a fixed temperature T: Recall that as T_c is approached from above, the leading eigenvalue $\lambda(T_c)$ drops below -1, so that $\lambda(T) \leqslant -1$ indicates an SC solution.
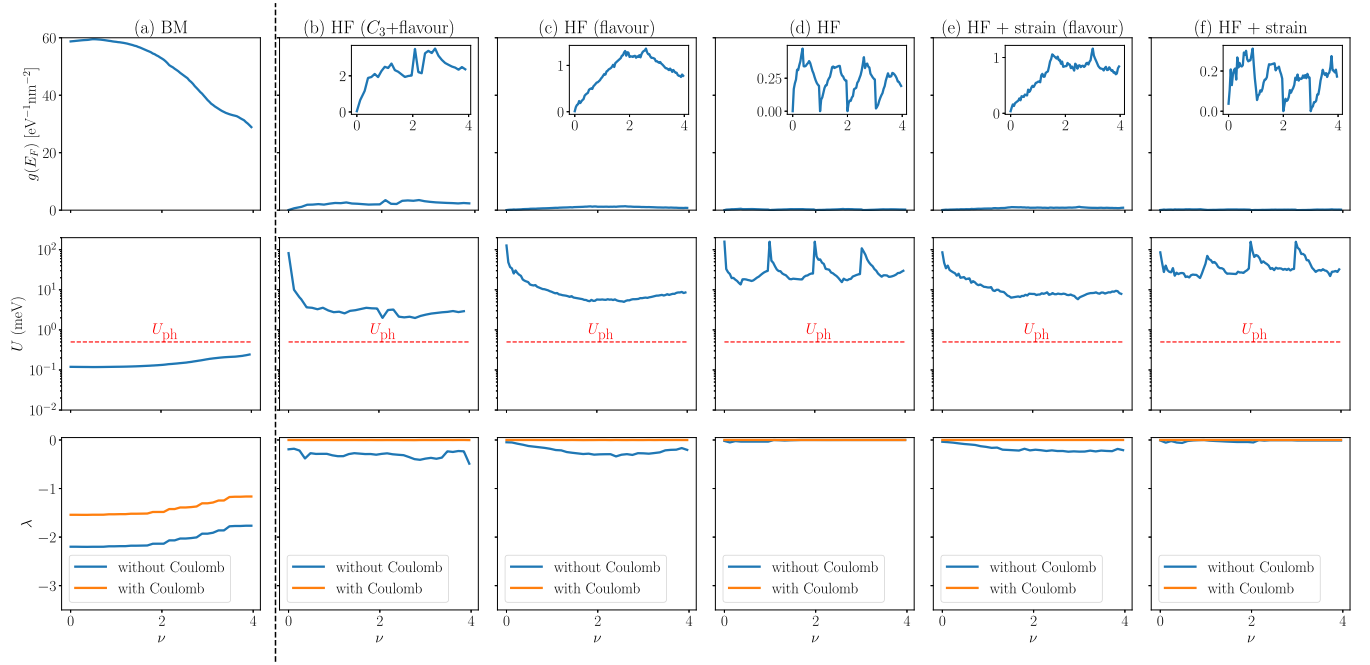
FIG. 1. Suppression of pairing by Coulomb interactions. Column (a) shows BM model results as a reference; columns [(b)–(d)] show results for unstrained HF-renormalized bands that respectively preserve both flavor and C_3 symmetry, only flavor, and break both; (e) and (f) show results for strained HF-renormalized bands with and without flavor symmetry (cf. Table I). Top row: Density of states at the Fermi level with a broadening corresponding to temperature $T = 2$ K. Middle row: Energy scales of the Thomas-Fermi screened Coulomb interaction $U = V(q = 0)$, and of the phonon-mediated attraction $U_{ph} = \frac{g}{A_M} = 0.5$ meV, where A_M is the moiré unit cell area. Even for the highest level of screening, $U \gg U_{ph}$, suppressing SC. Bottom row: Gap equation eigenvalue λ without and with Coulomb interactions at temperature $T = 2$ K, where $\lambda = -1$ signifies an SC instability. At the HF level, interactions reduce λ by more than an order of magnitude, reducing T_c well below the experimentally observed scale.

IV. RESULTS

The main results of this paper are summarized in Fig. 1, that shows the outcome of solving the gap equation starting with the HF-renormalized bands of several different physically motivated choices of parent state, listed in Table I and described below. Each column of Fig. 1 corresponds to a distinct choice of input band structure to the gap equation. As a function of doping, the top row shows the density of states, the middle row the energy scales of the K-phonon attraction (red, dashed) and the Thomas-Fermi screened Coulomb interaction (blue, solid), and the bottom row the results of solving the gap equation with (orange) and without (blue) including the screened Coulomb repulsion. In each case, we work at fixed $T = 2$ K, consistent with the typical T_c seen in experiment, and focus on positive fillings ν (i.e., the number of electrons per moiré unit cell relative to charge neutrality) due to the approximate particle-hole symmetry of the model.

First, Fig. 1(a) shows results for the noninteracting BM model. The sharp features of the BM bands are smeared out by the temperature, which is a larger energy scale than the bare bandwidth. For $T = 2$ K, $\lambda(T) < -1$, and hence there is SC at all ν even in the presence of the Coulomb interaction, consistent with previous computations on this model [32,33]. In the Supplemental Material [79] we show that for all fillings $\lambda(T) > -1$ at $T = 5$ K, hence the (filling-dependent) T_c for the BM bands lies between 2 and 5 K for our choice of parameters.

Figures 1(b)–1(d) show the results of incorporating HF renormalization for unstrained TBG with differing degrees of symmetry breaking. In Fig. 1(b), we perform HF on the bands, resulting in a broadened bandwidth, but preserve the full symmetries of the BM model. In Fig. 1(c), we allow the breaking of C_3 symmetry but preserve flavor symmetry. This allows us to access a metastable nematic (semi)metal [80]. This (semi)metal is the closest competitor to the strong-coupling insulators at zero strain (and becomes the ground state at $\nu = 0$ for modest strains comparable to those seen in experiments [49–51]—see below). Hence it is likely the relevant gapless parent state for SC when the correlated insulators are suppressed by strain [55] or disorder [81]. In Fig. 1(d), we allow both C_3 and flavor symmetries to break spontaneously, allowing gapped "generalized ferromagnets" at integer ν.

Figures 1(e) and 1(f) show results for the HF-renormalized bands of TBG subject to 0.3% heterostrain (which explicitly breaks C_3 and is known to stabilize a semimetallic state at $\nu = 0$ [55]) both with and without flavor symmetry. When flavor symmetry is preserved, the ground state at nonzero integer ν remains gapless, but on allowing flavor symmetry breaking it is the "incommensurate Kekulé spiral" state, which is gapped at $\nu = 2, 3$ and is gapless at $\nu = 1$ [56,57].

The bandwidth in each case [Figs. 1(b)–1(f)] is significantly broadened relative to the bare BM model and is typically on the order of 30 meV. (Quantum Monte Carlo at charge neutrality for the unstrained model [75] finds a similar bandwidth.) The enhanced bandwidth results in a suppression
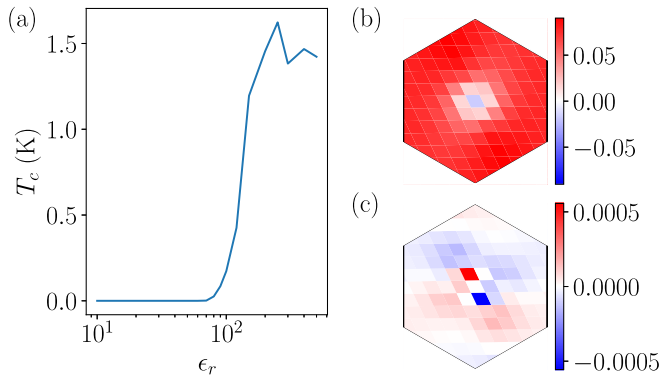
FIG. 2. Interaction dependence of T_c and symmetry of the gap function. (a) As the Coulomb interaction is reduced by increasing ϵ_r, T_c increases to around 2 K. T_c only reaches the experimental value of around 2 K for an unrealistically weak Coulomb interaction with $\epsilon_r > 100$. (b), (c) mBZ-even and mBZ-odd components of the gap function. All results are for filling $\nu = 2.48$.

of the density of states by nearly two orders of magnitude in Figs. 1(b)–1(f), which is reflected in a significantly stronger Coulomb repulsion due to the lowered screening. The two effects—suppression of the density of states and reduced screening—are both strongly antagonistic to K-phonon SC, as reflected by the dramatic change in the gap eigenvalue on their inclusion: A 2 K SC is ruled out in all cases [Figs. 1(b)–1(f)]. Given the exponential dependence of the gap eigenvalue λ on T, these results indicate that phonon-mediated/Thomas-Fermi screened SC mechanisms would yield T_c's well below the experimentally observed values. This conclusion holds irrespective of the choice of parent state, suggesting that the key mechanism that suppresses SC is the Coulomb-driven band unflattening. Each choice of parent state yields a distinct sequence of Lifshitz transitions and van Hove singularities (see Supplemental Material [79]). These features lead to doping-dependent modulations of the gap eigenvalue, but on a scale much lower than the overall suppression due to enhanced bandwidth.

One route to stabilize a K-phonon-mediated SC is to suppress the Coulomb scale by screening, which can be adjusted by changing the distance to a metallic back gate. Figure 2 shows more detailed results at $\nu = 2.48$ (close to the peak of the SC dome seen in many experiments) for the C_3-breaking, flavor-symmetric state studied in Fig. 1(c). Figure 2(a) shows the effect of tuning interactions via the relative permittivity ϵ_r, which enters the calculation in two ways. First, it controls the HF renormalization of the band structure, which reduces to the noninteracting BM bands as $\epsilon_r \to \infty$. Second, ϵ_r appears directly in the Coulomb interaction contribution to the BCS vertex in the gap equation: For $\epsilon_r \to \infty$ we recover a pure phonon-only attractive vertex. Both these effects tend to increase T_c when increasing ϵ_r. T_c is comparable to 2 K once $\epsilon_r > 100$. However, this is an unrealistically large value, as we would typically expect $\epsilon_r \sim 10$. Even including screening from the remote bands which we do not consider in our work, $\epsilon_r \lesssim 25$ [82]. Nevertheless, for completeness in Figs. 2(b) and 2(c) we show the mBZ-even and mBZ-odd components, respectively, of the leading gap function. Due to fermionic

anticommutation and the nontrivial action of inversion, that exchanges the valley degree of freedom ($\mathcal{I} \propto \tau_x$), the gap structure is quite rich. An even-parity gap function (which is forced to be a spin singlet) can have both mBZ-even, valley-triplet and mBZ-odd, valley-singlet components. Similarly, an odd-parity (hence spin-triplet) gap function can involve both mBZ-odd, valley-triplet and mBZ-even, valley-singlet contributions [79].

V. DISCUSSION

Upon discovery of SC in TBG, immediate comparisons with high-temperature SC were drawn. In particular, the emergence of an SC dome upon doping a correlated insulator is reminiscent of the phase diagram of the cuprates. However, recent work has shown that the correlated insulator is a symmetry-broken state quite unlike the Mott insulator in the cuprates [57,73]. Despite this, T_c in TBG is high compared to the Fermi temperature T_F ($T_c/T_F \sim 0.1$ [2]) and therefore the mechanism behind SC remains a matter of debate. STM measurements support a nodal gap [7], which requires non-s-wave pairing (or some topological obstruction [43]), often viewed as a hallmark of unconventional SC. Despite this, proposals of BCS-like phonon-mediated SC abound in the literature, typically resolving the apparent conflict between a BCS-like mechanism and large T_c/T_F by solving the gap equation for the narrow-bandwidth magic-angle BM model. The high density of states in the flat bands compensates for the very low density of free electrons in doped TBG, leading to T_c's comparable to experiment. However, it is likely that many of these studies substantially underestimate the bandwidth: There is both theoretical and experimental evidence that effects such as strain and interaction renormalization introduce substantial dispersion so that the bands are not really flat. We show that for such interaction-broadened bands, an SC calculation based on pairing from a specific optical phonon mode ("K phonon") leads to a T_c far below the experimental values. Other purely phonon-mediated mechanisms likely suffer similar problems.

At minimum, future studies of SC should incorporate Coulomb interactions beyond the simple Thomas-Fermi approximation employed here. For acoustic phonons retardation effects are important and the Anderson-Morel mechanism [77] can suppress the Coulomb repulsion [37]. The Anderson-Morel screening mechanism includes the screening from the electronic degrees of freedom with energies between the Debye frequency ω_D and the electronic bandwidth W. However, in our case we have an optical phonon with frequency $\omega_0 \gg W$ and therefore this mechanism is not active. Furthermore, already at the RPA level it is possible for Coulomb interactions to develop an attractive component [9,24,29,76]. The "heavy fermion" picture of TBG [83] may also lead to a more intricate interplay of electron-electron and electron-phonon interactions.

Experiments observe a relatively modest suppression of T_c on increasing screening, but a dramatic suppression of the correlated insulators. While a purely phonon-mediated attraction should show a significant T_c enhancement as the Coulomb repulsion is suppressed, a purely Coulomb-driven pairing should show a significant T_c suppression. Thus, we conclude that the situation is likely more complicated and

the attractive interaction may involve contributions from both phonons and Coulomb interactions.

[1] W. Kohn and J. M. Luttinger, New mechanism for superconductivity, Phys. Rev. Lett. **15**, 524 (1965).

[2] Y. Cao, V. Fatemi, S. Fang, K. Watanabe, T. Taniguchi, E. Kaxiras, and P. Jarillo-Herrero, Unconventional superconductivity in magic-angle graphene superlattices, Nature (London) **556**, 43 (2018).

[3] M. Yankowitz, S. Chen, H. Polshyn, Y. Zhang, K. Watanabe, T. Taniguchi, D. Graf, A. F. Young, and C. R. Dean, Tuning superconductivity in twisted bilayer graphene, Science **363**, 1059 (2019).

[4] X. Lu, P. Stepanov, W. Yang, M. Xie, M. A. Aamir, I. Das, C. Urgell, K. Watanabe, T. Taniguchi, G. Zhang, A. Bachtold, A. H. MacDonald, and D. K. Efetov, Superconductors, orbital magnets and correlated states in magic-angle bilayer graphene, Nature (London) **574**, 653 (2019).

[5] Y. Cao, V. Fatemi, A. Demir, S. Fang, S. L. Tomarken, J. Y. Luo, J. D. Sanchez-Yamagishi, K. Watanabe, T. Taniguchi, E. Kaxiras, R. C. Ashoori, and P. Jarillo-Herrero, Correlated insulator behaviour at half-filling in magic-angle graphene superlattices, Nature (London) **556**, 80 (2018).

[6] H. S. Arora, R. Polski, Y. Zhang, A. Thomson, Y. Choi, H. Kim, Z. Lin, I. Z. Wilson, X. Xu, J.-H. Chu, K. Watanabe, T. Taniguchi, J. Alicea, and S. Nadj-Perge, Superconductivity in metallic twisted bilayer graphene stabilized by WSe$_2$, Nature (London) **583**, 379 (2020).

[7] M. Oh, K. P. Nuckolls, D. Wong, R. L. Lee, X. Liu, K. Watanabe, T. Taniguchi, and A. Yazdani, Evidence for unconventional superconductivity in twisted bilayer graphene, Nature (London) **600**, 240 (2021).

[8] Y. Cao, D. Rodan-Legrain, J. M. Park, N. F. Q. Yuan, K. Watanabe, T. Taniguchi, R. M. Fernandes, L. Fu, and P. Jarillo-Herrero, Nematicity and competing orders in superconducting magic-angle graphene, Science **372**, 264 (2021).

[9] T. Cea and F. Guinea, Coulomb interaction, phonons, and superconductivity in twisted bilayer graphene, Proc. Natl. Acad. Sci. USA **118**, e2107874118 (2021).

[10] E. Khalaf, S. Chatterjee, N. Bultinck, M. P. Zaletel, and A. Vishwanath, Charged skyrmions and topological origin of superconductivity in magic-angle graphene, Sci. Adv. **7**, eabf5299 (2021).

[11] G. Sharma, M. Trushin, O. P. Sushkov, G. Vignale, and S. Adam, Superconductivity from collective excitations in magic-angle twisted bilayer graphene, Phys. Rev. Res. **2**, 022040(R) (2020).

[12] B. Roy and V. Juričić, Unconventional superconductivity in nearly flat bands in twisted bilayer graphene, Phys. Rev. B **99**, 121407(R) (2019).

[13] H. Isobe, N. F. Q. Yuan, and L. Fu, Unconventional superconductivity and density waves in twisted bilayer graphene, Phys. Rev. X **8**, 041041 (2018).

[14] T. Huang, L. Zhang, and T. Ma, Antiferromagnetically ordered Mott insulator and $d + id$ superconductivity in twisted bilayer graphene: A quantum Monte Carlo study, Sci. Bull. **64**, 310 (2019).

[15] D. M. Kennes, J. Lischner, and C. Karrasch, Strong correlations and $d + id$ superconductivity in twisted bilayer graphene, Phys. Rev. B **98**, 241407(R) (2018).

[16] H. C. Po, L. Zou, A. Vishwanath, and T. Senthil, Origin of Mott insulating behavior and superconductivity in twisted bilayer graphene, Phys. Rev. X **8**, 031089 (2018).

[17] M. Christos, S. Sachdev, and M. S. Scheurer, Nodal band-off-diagonal superconductivity in twisted graphene superlattices, Nat. Commun. **14**, 7134 (2023).

[18] M. Christos, S. Sachdev, and M. S. Scheurer, Superconductivity, correlated insulators, and Wess–Zumino–Witten terms in twisted bilayer graphene, Proc. Natl. Acad. Sci. USA **117**, 29543 (2020).

[19] S. Chatterjee, N. Bultinck, and M. P. Zaletel, Symmetry breaking and skyrmionic transport in twisted bilayer graphene, Phys. Rev. B **101**, 165141 (2020).

[20] E. Khalaf, P. Ledwith, and A. Vishwanath, Symmetry constraints on superconductivity in twisted bilayer graphene: Fractional vortices, $4e$ condensates, or nonunitary pairing, Phys. Rev. B **105**, 224508 (2022).

[21] Y.-Z. You and A. Vishwanath, Superconductivity from valley fluctuations and approximate SO(4) symmetry in a weak coupling theory of twisted bilayer graphene, npj Quantum Mater. **4**, 16 (2019).

[22] D. V. Chichinadze, L. Classen, and A. V. Chubukov, Nematic superconductivity in twisted bilayer graphene, Phys. Rev. B **101**, 224513 (2020).

[23] Y. Wang, J. Kang, and R. M. Fernandes, Topological and nematic superconductivity mediated by ferro-SU(4) fluctuations in twisted bilayer graphene, Phys. Rev. B **103**, 024506 (2021).

[24] J. González and T. Stauber, Kohn-Luttinger superconductivity in twisted bilayer graphene, Phys. Rev. Lett. **122**, 026801 (2019).

[25] V. Kozii, H. Isobe, J. W. F. Venderbos, and L. Fu, Nematic superconductivity stabilized by density wave fluctuations: Possible application to twisted bilayer graphene, Phys. Rev. B **99**, 144507 (2019).

[26] C.-C. Liu, L.-D. Zhang, W.-Q. Chen, and F. Yang, Chiral spin density wave and $d + id$ superconductivity in the magic-angle-twisted bilayer graphene, Phys. Rev. Lett. **121**, 217001 (2018).

[27] M. Fidrysiak, M. Zegrodnik, and J. Spałek, Unconventional topological superconductivity and phase diagram for an effective two-orbital model as applied to twisted bilayer graphene, Phys. Rev. B **98**, 085436 (2018).

[28] J. Ingham, T. Li, M. S. Scheurer, and H. D. Scammell, Quadratic Dirac fermions and the competition of ordered states in twisted bilayer graphene, arXiv:2308.00748.

[29] J. Gonzalez and T. Stauber, Universal mechanism of Ising superconductivity in twisted bilayer, trilayer and quadrilayer graphene, arXiv:2303.00583.

[30] C. Lewandowski, S. Nadj-Perge, and D. Chowdhury, Does filling-dependent band renormalization aid pairing in twisted bilayer graphene? npj Quantum Mater. **6**, 82 (2021).

[31] C. Lewandowski, D. Chowdhury, and J. Ruhman, Pairing in magic-angle twisted bilayer graphene: Role of phonon and plasmon umklapp, Phys. Rev. B **103**, 235401 (2021).

[32] F. Wu, A. H. MacDonald, and I. Martin, Theory of phonon-mediated superconductivity in twisted bilayer graphene, Phys. Rev. Lett. **121**, 257001 (2018).

[33] C.-X. Liu, Y. Chen, A. Yazdani, and B. A. Bernevig, Electron-K-phonon interaction in twisted bilayer graphene, arXiv:2303.15551.

[34] B. Lian, Z. Wang, and B. A. Bernevig, Twisted bilayer graphene: A phonon-driven superconductor, Phys. Rev. Lett. **122**, 257002 (2019).

[35] F. Wu, E. Hwang, and S. Das Sarma, Phonon-induced giant linear-in-T resistivity in magic angle twisted bilayer graphene: Ordinary strangeness and exotic superconductivity, Phys. Rev. B **99**, 165112 (2019).

[36] T. J. Peltonen, R. Ojajärvi, and T. T. Heikkilä, Mean-field theory for superconductivity in twisted bilayer graphene, Phys. Rev. B **98**, 220504(R) (2018).

[37] G. Shavit, E. Berg, A. Stern, and Y. Oreg, Theory of correlated insulators and superconductivity in twisted bilayer graphene, Phys. Rev. Lett. **127**, 247703 (2021).

[38] F. Schrodi, A. Aperis, and P. M. Oppeneer, Prominent Cooper pairing away from the Fermi level and its spectroscopic signature in twisted bilayer graphene, Phys. Rev. Res. **2**, 012066(R) (2020).

[39] A. Blason and M. Fabrizio, Local Kekulé distortion turns twisted bilayer graphene into topological Mott insulators and superconductors, Phys. Rev. B **106**, 235112 (2022).

[40] Y. W. Choi and H. J. Choi, Strong electron-phonon coupling, electron-hole asymmetry, and nonadiabaticity in magic-angle twisted bilayer graphene, Phys. Rev. B **98**, 241412(R) (2018).

[41] F. Wu, Topological chiral superconductivity with spontaneous vortices and supercurrent in twisted bilayer graphene, Phys. Rev. B **99**, 195114 (2019).

[42] F. Wu and S. Das Sarma, Identification of superconducting pairing symmetry in twisted bilayer graphene using in-plane magnetic field and strain, Phys. Rev. B **99**, 220507(R) (2019).

[43] J. Yu, Y.-A. Chen, and S. Das Sarma, Euler-obstructed Cooper pairing: Nodal superconductivity and hinge Majorana zero modes, Phys. Rev. B **105**, 104515 (2022).

[44] Y. Saito, J. Ge, K. Watanabe, T. Taniguchi, and A. F. Young, Independent superconductors and correlated insulators in twisted bilayer graphene, Nat. Phys. **16**, 926 (2020).

[45] P. Stepanov, I. Das, X. Lu, A. Fahimniya, K. Watanabe, T. Taniguchi, F. H. L. Koppens, J. Lischner, L. Levitov, and D. K. Efetov, Untying the insulating and superconducting orders in magic-angle graphene, Nature (London) **583**, 375 (2020).

[46] X. Liu, Z. Wang, K. Watanabe, T. Taniguchi, O. Vafek, and J. I. A. Li, Tuning electron correlation in magic-angle twisted bilayer graphene using Coulomb screening, Science **371**, 1261 (2021).

[47] C. Chen, K. P. Nuckolls, S. Ding, W. Miao, D. Wong, M. Oh, R. L. Lee, S. He, C. Peng, D. Pei, Y. Li, S. Zhang, J. Liu, Z. Liu, C. Jozwiak, A. Bostwick, E. Rotenberg, C. Li, X. Han, D. Pan, X. Dai, C. Liu, B. A. Bernevig, Y. Wang, A. Yazdani, and Y. Chen, Strong inter-valley electron-phonon coupling in magic-angle twisted bilayer graphene, arXiv:2303.14903.

[48] R. Bistritzer and A. H. MacDonald, Moiré bands in twisted double-layer graphene, Proc. Natl. Acad. Sci. USA **108**, 12233 (2011).

[49] A. Kerelsky, L. J. McGilly, D. M. Kennes, L. Xian, M. Yankowitz, S. Chen, K. Watanabe, T. Taniguchi, J. Hone, C. Dean, A. Rubio, and A. N. Pasupathy, Maximized electron interactions at the magic angle in twisted bilayer graphene, Nature (London) **572**, 95 (2019).

[50] Y. Xie, B. Lian, B. Jäck, X. Liu, C.-L. Chiu, K. Watanabe, T. Taniguchi, B. A. Bernevig, and A. Yazdani, Spectroscopic signatures of many-body correlations in magic-angle twisted bilayer graphene, Nature (London) **572**, 101 (2019).

[51] Y. Choi, J. Kemmer, Y. Peng, A. Thomson, H. Arora, R. Polski, Y. Zhang, H. Ren, J. Alicea, G. Refael, F. von Oppen, K. Watanabe, T. Taniguchi, and S. Nadj-Perge, Electronic correlations in twisted bilayer graphene near the magic angle, Nat. Phys. **15**, 1174 (2019).

[52] Y. Jiang, X. Lai, K. Watanabe, T. Taniguchi, K. Haule, J. Mao, and E. Y. Andrei, Charge order and broken rotational symmetry in magic-angle twisted bilayer graphene, Nature (London) **573**, 91 (2019).

[53] S. L. Tomarken, Y. Cao, A. Demir, K. Watanabe, T. Taniguchi, P. Jarillo-Herrero, and R. C. Ashoori, Electronic compressibility of magic-angle graphene superlattices, Phys. Rev. Lett. **123**, 046601 (2019).

[54] S. Lisi, X. Lu, T. Benschop, T. A. de Jong, P. Stepanov, J. R. Duran, F. Margot, I. Cucchi, E. Cappelli, A. Hunter, A. Tamai, V. Kandyba, A. Giampietri, A. Barinov, J. Jobst, V. Stalman, M. Leeuwenhoek, K. Watanabe, T. Taniguchi, L. Rademaker, S. J. van der Molen, M. P. Allan, D. K. Efetov, and F. Baumberger, Observation of flat bands in twisted bilayer graphene, Nat. Phys. **17**, 189 (2021).

[55] D. E. Parker, T. Soejima, J. Hauschild, M. P. Zaletel, and N. Bultinck, Strain-induced quantum phase transitions in magic-angle graphene, Phys. Rev. Lett. **127**, 027601 (2021).

[56] G. Wagner, Y. H. Kwan, N. Bultinck, S. H. Simon, and S. A. Parameswaran, Global phase diagram of the normal state of twisted bilayer graphene, Phys. Rev. Lett. **128**, 156401 (2022).

[57] Y. H. Kwan, G. Wagner, T. Soejima, M. P. Zaletel, S. H. Simon, S. A. Parameswaran, and N. Bultinck, Kekulé spiral order at all nonzero integer fillings in twisted bilayer graphene, Phys. Rev. X **11**, 041063 (2021).

[58] X. Wang, J. Finney, A. L. Sharpe, L. K. Rodenbach, C. L. Hsueh, K. Watanabe, T. Taniguchi, M. A. Kastner, O. Vafek, and D. Goldhaber-Gordon, Unusual magnetotransport in twisted bilayer graphene from strain-induced open Fermi surfaces, Proc. Natl. Acad. Sci. USA **120**, e2307151120 (2023).

[59] Y. H. Kwan, G. Wagner, N. Chakraborty, S. H. Simon, and S. A. Parameswaran, Domain wall competition in the Chern insulating regime of twisted bilayer graphene, Phys. Rev. B **104**, 115404 (2021).

[60] Y. H. Kwan, G. Wagner, N. Bultinck, S. H. Simon, and S. A. Parameswaran, Skyrmions in twisted bilayer graphene: Stability, pairing, and crystallization, Phys. Rev. X **12**, 031020 (2022).

[61] N. Bultinck, E. Khalaf, S. Liu, S. Chatterjee, A. Vishwanath, and M. P. Zaletel, Ground state and hidden symmetry of magic-angle graphene at even integer filling, Phys. Rev. X **10**, 031034 (2020).

[62] B. A. Bernevig, Z.-D. Song, N. Regnault, and B. Lian, Twisted bilayer graphene. III. Interacting Hamiltonian and exact symmetries, Phys. Rev. B **103**, 205413 (2021).

[63] B. Lian, Z.-D. Song, N. Regnault, D. K. Efetov, A. Yazdani, and B. A. Bernevig, Twisted bilayer graphene. IV. Exact insulator ground states and phase diagram, Phys. Rev. B **103**, 205414 (2021).

[64] K. Hejazi, X. Chen, and L. Balents, Hybrid Wannier Chern bands in magic angle twisted bilayer graphene and the quantized anomalous Hall effect, Phys. Rev. Res. **3**, 013242 (2021).

[65] M. Xie and A. H. MacDonald, Nature of the correlated insulator states in twisted bilayer graphene, Phys. Rev. Lett. **124**, 097601 (2020).

[66] S. Liu, E. Khalaf, J. Y. Lee, and A. Vishwanath, Nematic topological semimetal and insulator in magic-angle bilayer graphene at charge neutrality, Phys. Rev. Res. **3**, 013033 (2021).

[67] Y. Zhang, K. Jiang, Z. Wang, and F. Zhang, Correlated insulating phases of twisted bilayer graphene at commensurate filling fractions: A Hartree-Fock study, Phys. Rev. B **102**, 035136 (2020).

[68] J. Liu and X. Dai, Theories for the correlated insulating states and quantum anomalous Hall effect phenomena in twisted bilayer graphene, Phys. Rev. B **103**, 035427 (2021).

[69] T. Cea, P. A. Pantaleón, N. R. Walet, and F. Guinea, Electrostatic interactions in twisted bilayer graphene, Nano Mater. Sci. **4**, 27 (2022).

[70] T. Cea and F. Guinea, Band structure and insulating states driven by Coulomb interaction in twisted bilayer graphene, Phys. Rev. B **102**, 045107 (2020).

[71] F. Xie, N. Regnault, D. Călugăru, B. A. Bernevig, and B. Lian, Twisted symmetric trilayer graphene. II. Projected Hartree-Fock study, Phys. Rev. B **104**, 115167 (2021).

[72] Y. H. Kwan, G. Wagner, N. Bultinck, S. H. Simon, E. Berg, and S. A. Parameswaran, Electron-phonon coupling and competing Kekulé orders in twisted bilayer graphene, arXiv:2303.13602.

[73] K. P. Nuckolls, R. L. Lee, M. Oh, D. Wong, T. Soejima, J. P. Hong, D. Călugăru, J. Herzog-Arbeitman, B. A. Bernevig, K. Watanabe, T. Taniguchi, N. Regnault, M. P. Zaletel, and A. Yazdani, Quantum textures of the many-body wavefunctions in magic-angle graphene, Nature (London) **620**, 525 (2023).

[74] O. Vafek and J. Kang, Renormalization group study of hidden symmetry in twisted bilayer graphene with Coulomb interactions, Phys. Rev. Lett. **125**, 257602 (2020).

[75] J. S. Hofmann, E. Khalaf, A. Vishwanath, E. Berg, and J. Y. Lee, Fermionic Monte Carlo study of a realistic model of twisted bilayer graphene, Phys. Rev. X **12**, 011061 (2022).

[76] Z. A. H. Goodwin, F. Corsetti, A. A. Mostofi, and J. Lischner, Attractive electron-electron interactions from internal screening in magic-angle twisted bilayer graphene, Phys. Rev. B **100**, 235424 (2019).

[77] P. Morel and P. W. Anderson, Calculation of the superconducting state parameters with retarded electron-phonon interaction, Phys. Rev. **125**, 1263 (1962).

[78] V. Bach, E. H. Lieb, and J. P. Solovej, Generalized Hartree-Fock theory and the Hubbard model, J. Stat. Phys. **76**, 3 (1994).

[79] See Supplemental Material at http://link.aps.org/supplemental/10.1103/PhysRevB.109.104504 for more details.

[80] This state is semimetallic at $\nu = 0$, while it is metallic at all other ν.

[81] K. Kolář, G. Shavit, C. Mora, Y. Oreg, and F. von Oppen, Anderson's theorem for correlated insulating states in twisted bilayer graphene, Phys. Rev. Lett. **130**, 076204 (2023).

[82] J. M. Pizarro, M. Rösner, R. Thomale, R. Valentí, and T. O. Wehling, Internal screening and dielectric engineering in magic-angle twisted bilayer graphene, Phys. Rev. B **100**, 161102(R) (2019).

[83] Z.-D. Song and B. A. Bernevig, Magic-angle twisted bilayer graphene as a topological heavy fermion problem, Phys. Rev. Lett. **129**, 047601 (2022).